Multiple-Quantum Nuclear Magnetic Resonance Spectroscopy

M. MUNOWITZ AND A. PINES

A nuclear magnetic resonance (NMR) event is popularly viewed as the flip of a single spin in a magnetic field, stimulated by the absorption or emission of only one quantum of radio-frequency energy. Nevertheless, resonances between nuclear spin states that differ by more than one unit in the Zeeman quantum number also can be induced in systems of coupled spins by suitably designed sequences of radio-frequency pulses. Pairs of states excited in this way oscillate coherently at the frequencies of the corresponding multiple-quantum transitions and produce a response that may be monitored indirectly in a two-dimensional time-domain experiment. The pattern of multiple-quantum excitation and response, influenced largely by the concerted interactions of groups of coupled nuclei, simplifies the NMR spectrum in some instances and provides significant new information in others. Applications of multiple-quantum NMR extend to problems in many different areas, ranging from studies of the structure and function of proteins and nucleic acids in solution to investigations of the arrangements of atoms in amorphous semiconductors. The specific spectroscopic techniques are varied as well and include methods designed, for example, to simplify spectral analysis for liquids and liquid crystals, eliminate inhomogeneous broadening, study interatomic connectivity in liquid-state molecules, identify clusters of atoms in solids, enhance the spatial resolution in solid-state imaging experiments, and probe correlated molecular motions.

LONG RECOGNIZED AS AN IMPORTANT TECHNIQUE FOR determining the structure of organic molecules, nuclear magnetic resonance (NMR) spectroscopy continues to find new applications in a variety of disciplines, providing data of increasing specificity about systems of increasing complexity. Among the many subjects now under investigation by NMR are problems in such diverse fields as materials science, geology, biochemistry, medicine, and physiology, all of which benefit from the atom-by-atom, noninvasive probing of molecular structure and dynamics afforded by magnetic resonance techniques. Experimental methods may differ, depending on the specific problems to be solved, but most are designed to ascertain, through the resonances of individual spins, the magnitudes and directions of magnetic fields in the vicinity of selected nuclei. Equipped with a knowledge of the microscopic origin of the local field at a site, together with an understanding of the dependence of this field on structural and electronic parameters, the spectroscopist is able first to locate and identify a nuclear position and then to develop a physical picture of its immediate environment. Connections between atoms, interatomic distances and angles, and motions of molecules or portions of molecules are revealed in this manner, with spatial resolution often approaching hundredths of angstroms and temporal resolution ranging from seconds to microseconds. Relations between positions, arising either from magnetic spin-spin couplings or from a physical exchange of the nuclei between sites, become apparent as well in certain experiments; other techniques provide a picture of the long-range spatial distribution of the nuclei, from which an image of the macroscopic structure of the material can be constructed.

Supporting these experiments is a collection of techniques designed to shape and simplify the NMR spectrum by taking control of the local fields and interactions that govern the system (*1*). One of these methods, multiple-quantum spectroscopy, takes NMR beyond the simple resonance of a single spin in a local field and engineers instead the collective excitation and response of a group of coupled spins (*2–5*). This extension widens the range of applications of NMR by solving several long-standing spectroscopic problems associated with conventional techniques and, accordingly, can be best understood by first considering some of the basic phenomena common to all magnetic resonance experiments.

Single-Quantum Excitation and the Local Field Model

Differences in aims and methods notwithstanding, an NMR experiment typically begins with an ensemble of independent spins, each with its own elementary magnetic moment, existing in equilibrium in a considerably larger external magnetic field. The basic pattern of energy levels is established by the static coupling of the nuclear magnetic moments with the external, or Zeeman, field, and a fine structure arises from similar interactions with the much smaller internal fields. Perturbed from equilibrium by one or more pulses of electromagnetic radiation, the system of spins responds by oscillating at its natural frequencies as it attempts to return to a stationary state. Both the spectrum of frequencies exhibited during the period of response as well as the time scale over which the recovery takes place supply information about the static and fluctuating magnetic fields in the sample (*6, 7*).

The simplest example of these general principles is found in the response of a system of spin-1/2 nuclei, such as ^{1}H, ^{15}N, ^{13}C, ^{29}Si, or ^{31}P, to a single intense pulse of a resonant radio-frequency (RF) field. Before the pulse the nuclear magnetic moments are oriented either parallel or antiparallel to the direction of the external field,

---

M. Munowitz is a research chemist at Amoco Research Center, Naperville, IL 60566. A. Pines is professor of chemistry at the University of California, Berkeley, and faculty senior scientist at the Lawrence Berkeley Laboratory, Berkeley, CA 94720.

about which they precess, with uncorrelated phases, at angular frequencies determined by the total field present at each site. These asynchronous oscillations are damped out over the ensemble, leaving just a time-independent macroscopic magnetic moment that reflects the slight energetic preference of the spins for one of the two allowed orientations, usually the one parallel to the external field. The condition of the system at equilibrium is illustrated schematically in Fig. 1, where vectors depict the uncorrelated motions of the expectation values of the individual nuclear moments. Only when "tipped" by the pulse do the spins exhibit a phase coherence and thus appear to precess synchronously, developing in the process a time-dependent macroscopic magnetic moment transverse to the external field. The oscillations of this magnetization produce magnetic dipole radiation, observable as a time-varying induced voltage in a receiving coil tuned to the nuclear frequencies.

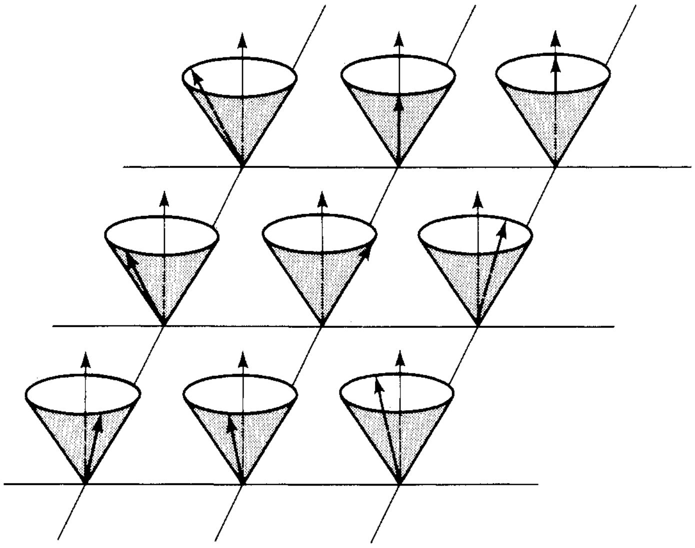

Fig. 1. Ensemble of spin-1/2 nuclei in thermal equilibrium in an external magnetic field. In the absence of internal interactions the magnetic moments precess about the Zeeman field at the same frequency but with random phases, thus averaging to zero the macroscopic component transverse to the axis of precession.

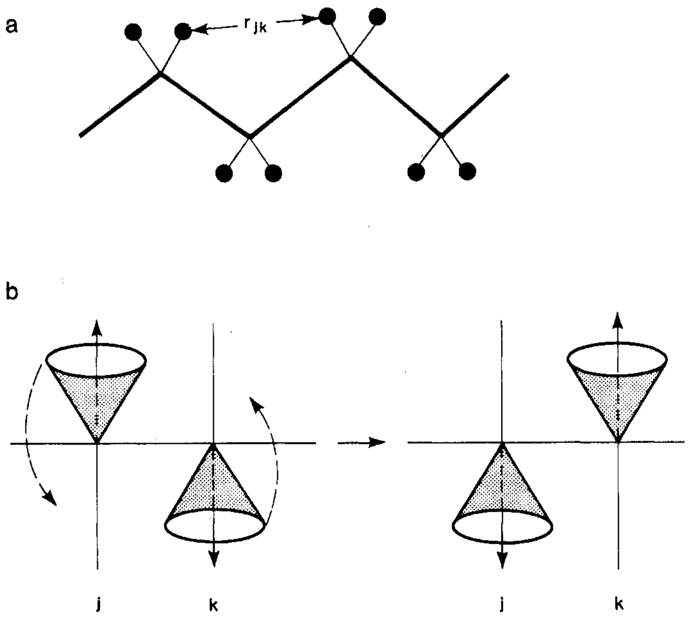

Fig. 2. Classical interaction of two nuclear magnetic dipoles. (a) Internuclear geometry. The magnitude of the dipolar field depends on the length and orientation of the internuclear vector, **r**, and the sign depends on the alignment of the source spin with respect to the external field. (b) The time-dependent component perpendicular to the axis of precession acts in the same fashion as a rotating RF field, bringing about an energy conserving mutual reorientation, or "flip-flop," when the natural frequencies of the interacting spins are sufficiently close.

Two principal magnetic interactions, the chemical shift and the spin-spin coupling, ultimately define the energy levels of a spin-1/2 system and thereby determine its spectrum (*8*). The chemical shift, or shielding, interaction alters the magnitude and direction of the external magnetic field through an interplay with fields produced by the orbital motion of the electrons surrounding each nucleus. The effect is different at each chemically inequivalent site and involves only one spin at a time. By contrast, the direct through-space coupling of the magnetic moment of one nucleus with the dipolar field of a neighboring magnetic moment necessarily involves two spins at once and provides a mechanism by which two initially independent spins can communicate. The magnitude of a local dipolar field varies both with the distance from the source and with the orientation relative to the Zeeman field, falling off as

$$\frac{1}{2}\,(3\cos^2\theta_{jk} - 1)/r_{jk}^3$$

where r_{jk} denotes the length of the vector from nucleus j to nucleus k and where θ_{jk} denotes the angle between the internuclear vector and the external field. Precessing either up or down, as suggested in Fig. 2, one magnetic moment increases or decreases the net static field at a distant location, generating at the same time a rotating component that can reorient a neighboring moment in a resonant process analogous to the action of an external RF field. Another form of spin-spin coupling, propagated indirectly through the electrons in chemical bonds, also exists and connects nuclei in the same fashion but usually with local fields far smaller in magnitude. This indirect interaction, also known as *J* coupling, plays an important role in the NMR of isotropic phases, where molecular motion averages the angular dependence of the direct dipole-dipole interaction to zero.

Difficulties with Conventional NMR Methods

Governed completely by the well-defined magnetic interactions described above, an NMR spectrum will yield, at least in principle, the desired structural information through an analysis of the positions, intensities, and widths of the resonances; in practice, however, a successful interpretation is contingent upon the degree to which the sources of the local fields can be limited to a manageable number. An example of the problems that may develop with a simple local field interpretation is provided by the spectrum shown in Fig. 3 (*9*), where it is evident that the response of even a relatively small system of eight hydrogen nuclei is already perhaps too complicated to be understood by a conventional analysis. The resolution is degraded not by the intrinsic widths of the individual resonances, which are three to four orders of magnitude narrower than that of the overall spectrum, but rather by the large number of resonances crowding into a limited range of frequencies. The number of lines is related directly to the number of distinct local field configurations that may be presented to any of the spins and therefore grows exponentially with the size of the system, running into the hundreds and thousands for simple molecules in anisotropic fluids and ultimately approaching infinity in polycrystalline solids. High-resolution spectra of molecules in isotropic phases, determined mostly by the *J* couplings, usually develop from smaller groups of spins, but nevertheless may also be complicated by overlapping signals from numerous distinct subunits. Hence the challenge faced by NMR spectroscopy today is to simplify the response of an arbitrarily complex system without sacrificing any important information contained therein.

Multiple-Quantum Excitation and Response

The goal of simplification in NMR is met most effectively by a class of highly specific pulse techniques designed to alter the local fields and interactions under which a system of spins evolves and thereby to extract a tailored response to an intentionally complicated pattern of excitation. This activist approach distinguishes NMR from most other methods of spectroscopy, in which energy levels and interactions usually must be probed passively, without modification or tampering. The extent of external manipulation exercised in NMR depends on the aim of the experiment at hand, and the actions required may range from the addition of just one extra pulse, perhaps to generate a spin echo (*10, 11*), to the incorporation of lengthy cycles of pulses in order to eliminate the effects of the homonuclear dipole-dipole coupling (*12*).

Formulated in this spirit of intervention and control, multiple-quantum excitation addresses the problem of complexity in the NMR response by forcing a group of nuclei to react together to an intrinsically simpler local field. The essential features of the approach are illustrated in Fig. 4, which suggests how a subset of the system is excited to create a collective nonequilibrium state, a coupled "super-spin," which subsequently oscillates at frequencies determined only by interactions with those spins remaining outside the group. As the number of spins inside increases, the number outside necessarily decreases, and with it so does the number of possible local field configurations and their associated resonances. The effect is similar to that which follows the replacement of some of the nuclei in a molecule by nonmagnetic isotopes or species with significantly different resonant frequencies, for both multiple-quantum excitation and chemical substitution effectively label and set aside a portion of the system apart from the whole (*13*).

Multiple-quantum excitation is generally achieved with a series of RF pulses designed to act together with the spin-spin couplings naturally present in the system. Viewed quantum mechanically, the effect of the interaction between the spins and n quanta of electromagnetic radiation is to establish a coherent superposition of spin states for which the magnetic quantum numbers differ by n units.

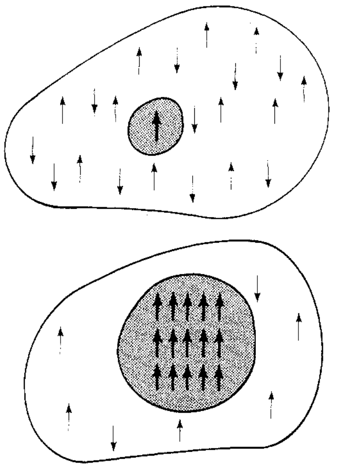

Fig. 4. Idealized conception of single-quantum and multiple-quantum excitation. In conventional NMR, a spin is excited independently and allowed to precess in the local fields of its neighbors, thereby, developing a time-dependent macroscopic magnetic moment. In multiple-quantum NMR a group of spins, excited collectively, responds to the local field of the unexcited "spectator" spins without emitting observable dipole radiation.

Each nonstationary mode so created oscillates at the transition frequency spanning the two connected states, so the apparent result is equivalent to a net absorption or emission of n quanta, but, unlike the response of a conventionally excited single-quantum mode, the coherent n-quantum oscillations do not produce magnetic dipole radiation. Accordingly, the time-dependent multipole moments that correspond to the multiple-quantum transitions remain invisible to any conventional dipole antenna normally used to detect single-quantum resonances. Observation of these nominally forbidden modes instead must be made indirectly according to the two-dimensional experimental design laid out in the block diagram shown in Fig. 5 (*14*). Under this scheme, multiple-quantum excitation is applied for a time τ during the initial period U, which is followed immediately by a hidden response for a time t_1. The oscillations of the system are then halted, and an additional period of excitation, V, applied for a time τ' is used to generate a dipole-allowed mode spanning two levels for which $n = \pm 1$. The oscillations of these connected states, taken two at a time from the multilevel system, produce observable dipole radiation formally analogous to that resulting from coherent precession in a simple system of independent spins-1/2 (*15, 16*). The signal is monitored by conventional means in a series of experiments in which the duration of the multiple-quantum evolution period is increased incrementally. The single-quantum signal obtained in this manner is

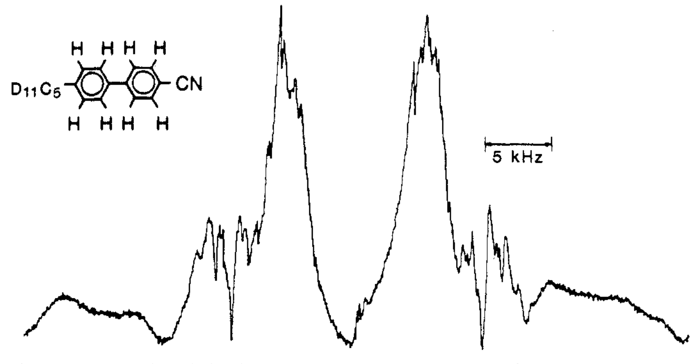

Fig. 3. Conventional single-quantum NMR spectrum of a partially oriented system of eight spins, the hydrogen nuclei in the biphenyl portion of the nematic liquid crystal 4-cyano-4′-n-pentyl-d_{11}-biphenyl (*9*). Dipole-dipole couplings between spins on different molecules are averaged to zero owing to translational diffusion, leaving the spectrum determined primarily by intramolecular interactions. The single-quantum transitions proliferate in the presence of the numerous potential configurations of the independent dipolar fields, enriching the spectrum but at the same time impeding a simple analysis. [Reprinted from (*9*) with permission © 1984 Taylor & Francis, Ltd.]

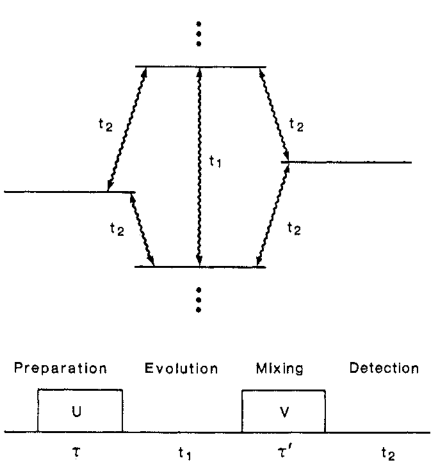

Fig. 5. Pulse sequence design for multiple-quantum spectroscopy. The system is excited to a nonstationary multiple-quantum condition during a preparation period, U, of duration τ. The subsequent response, invisible to a conventional magnetic dipole receiver, is halted after an evolution time, t_1, and converted to a single-quantum mode during a mixing period, V. The single-quantum oscillations detected during the second response period, t_2, provide an indirect view of the earlier multiple-quantum response. The section from a generic energy level diagram is intended to suggest how phase coherence between any pair of quantum states may be created and then transferred to an allowed single-quantum mode.

necessarily determined by the detailed multiple-quantum history of the spins up to the point of detection and provides a window through which the otherwise invisible degrees of freedom can be viewed.

Figure 6 demonstrates the principles of multiple-quantum spectroscopy with a set of n-quantum spectra recorded from the same eight-spin system responsible for the poorly resolved spectrum shown earlier in Fig. 3 (*9, 17*). Each cluster of resonances is associated with a net change by n of the total Zeeman quantum number, which takes on all integral values between 4 and -4, including 0. Local field shifts originating from single-spin interactions such as chemical shielding typically appear as various arithmetic combinations of components from all the nuclei actively involved, with any offset from resonance, $\Delta\omega$, common to all the spins showing up as $n\Delta\omega$ in the n-quantum spectra (*14, 18–20*). In a similar fashion, a shift by ϕ in the phase of the RF excitation sequence appears as $n\phi$ to each n-quantum component and serves to mix absorption and dispersion modes into each resonance with coefficients of $\cos(n\phi)$ and $\sin(n\phi)$ (*20*). Resonances within each spectrum of order n are shifted in frequency by the single-spin interactions and then split by the spin-spin interactions into multiplets in which the positions of the lines are determined by the different magnitudes of the residual local field.

Two important characteristics of the overall pattern are apparent at once:

1) The number of peaks belonging to a spectral order diminishes sharply as the number of quanta increases, reflecting the progressive simplification of the residual local field. The increase in resolution that results is not counterbalanced by any real loss of knowledge, however, since a system of N spins is completely specified by no more than $N(N - 1)/2$ spin-spin couplings, and the usually dense single-quantum spectrum contains mostly redundant information. In principle, the positions and intensities of the $(N - 1)$– and $(N - 2)$–quantum peaks are sufficient to yield a full set of dipolar coupling constants, from which the geometric structure of the system can be inferred.

2) The total integrated intensity of the lines within an order also diminishes sharply as the number of quanta increases, reflecting the decrease in the number of admissible combinations of states consistent with the net absorption or emission of n quanta. This loss of intensity is the price asked for the enhancement of resolution gained in the multiple-quantum spectrum, but methods of n-quantum selective excitation, whereby the total signal energy is channeled into resonances of just one order, are available to lessen the problem (*21, 22*). In general, however, simple combinatorial arguments show that the distribution of intensity over the different transition orders falls off roughly as a Gaussian distribution, proportional to $\exp(-n^2/N)$, with the variance of the curve related to the size of the system, N (*23*).

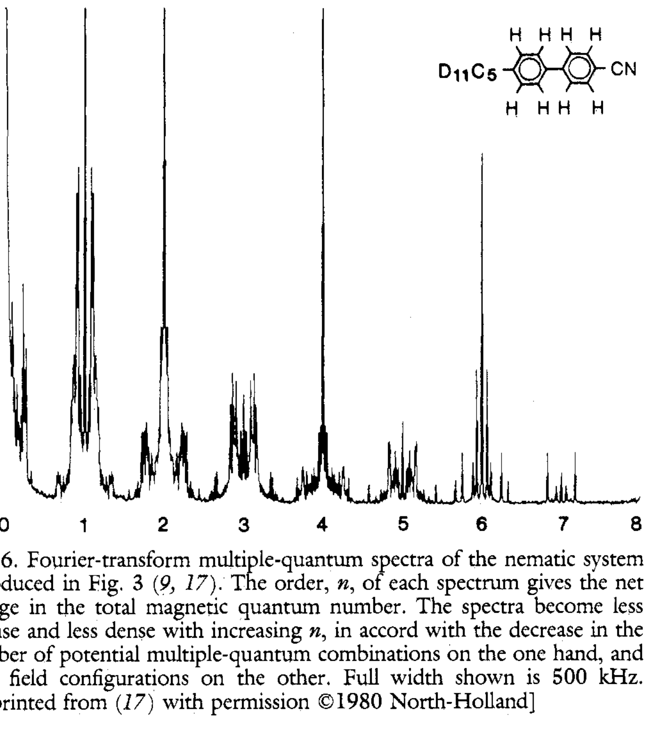

Fig. 6. Fourier-transform multiple-quantum spectra of the nematic system introduced in Fig. 3 (*9, 17*). The order, n, of each spectrum gives the net change in the total magnetic quantum number. The spectra become less intense and less dense with increasing n, in accord with the decrease in the number of potential multiple-quantum combinations on the one hand, and local field configurations on the other. Full width shown is 500 kHz. [Reprinted from (*17*) with permission ©1980 North-Holland]

A barrier to collective excitation is encountered with the N-quantum transition, which occurs just between the one state in which all the spins are up and the one state in which all the spins are down. Having interacted with a full complement of N quanta, the N spins-1/2 can accept no more; any attempt to add another quantum will only decouple the system entirely. Moreover, with all N spins tied up in the N-quantum event, there are no external spins available to generate a local field, and the subsequent response therefore is unaffected by the spin-spin couplings. Hence the N-quantum spectrum is a single line, positioned at the sum of the chemical shifts of all N nuclei and the enhanced offset $N\Delta\omega$, without the multiple structure normally arising from the internuclear interactions (*24*).

Simplification of High-Resolution Spectra by Multiple-Quantum Filtering

The spectrum of a complex molecule in isotropic solution frequently is a mixture of relatively simple subspectra, each originating from a small, effectively closed subsystem defined by the through-bond J couplings. These subsystems may be manipulated directly by a number of multiple-quantum methods designed to isolate the response of selected groups of spins according to their sizes, coupling patterns, and average resonant frequencies. The intent throughout is to retain both the information of the complete spectrum and the simplicity of the constituent subspectra.

Many high-resolution multiple-quantum techniques specifically use the N-quantum excitation barrier to limit an edited spectrum to contributions from groups containing N spins or more. These methods simply restrict the signal observed during the detection period of a multiple-quantum experiment to components derived from former N-quantum modes. Since no fewer than N spin-1/2 nuclei can sustain the N-quantum coherence, selective observation of the N-quantum → single-quantum pathways effectively screens the total response through a high-pass filter with a cut-off point of N spins (*25–28*). Most filtering schemes of this sort use RF phase shifts to control the phases of the multiple-quantum oscillations and then combine the results of a series of experiments to bring about the desired destructive interference. An important modification of the basic method exploits the insensitivity of the N-quantum oscillation frequency to spin-spin couplings and chemical shift differences in order to set up a bandpass filter, which also rejects signals from groups containing more than N spins (*29, 30*). Additional fine tuning may be achieved as well through the incorporation of a topologically selective preparation period, under which only those subsystems sharing a desired coupling pattern are excited at the start of the sequence (*31, 32*). The latter methods distinguish groups that would otherwise pass through a straight multiple-quantum filter. For example, a four-spin system of the form AX_3, in which one spin A is weakly coupled to three magnetically equivalent spins X, can be made to look different from a four-spin system of the form A_2X_2, in which two equivalent spins are weakly coupled to two other equivalent spins.

Figures 7 and 8 give some idea of the spectroscopic advantages offered by spin filtration techniques. In both demonstrations, the two-dimensional data presentations make explicit the relationship between frequency components present during an initial response period and frequency components subsequently generated by a mixing process. The ^{13}C spectrum shown in Fig. 7, for example, identifies all double-quantum → single-quantum pathways in an organic molecule by a common double-quantum frequency along one of the axes (*33*). Any pair of single-quantum signals sharing this frequency is immediately recognized as originating from the same pair of coupled carbons. Analysis of all the connections revealed in this way permits the reconstruction of the entire carbon skeleton of the molecule, an important first step towards a complete understanding of the structure.

Relations between single-quantum frequencies ω_1 and ω_2 present during two separate response periods also provide information about spin-spin coupling and atomic connectivity in a molecule. In general, peaks on the diagonal ($\omega_1 = \omega_2$) of a single-quantum correlated spectrum arise from uncoupled nuclei, which oscillate at the same frequency during both periods; whereas peaks off the diagonal arise from coupled nuclei, interacting either through space or through bonds, which exchange frequencies during the mixing phase (*14*, *34*). Typically rich in information but often too complicated to be interpreted successfully, a two-dimensional spectrum of a large molecule can be simplified considerably by the use of both multiple-quantum filtering to reduce the intensities of the diagonal peaks and topological filtering to isolate signals from designated spin patterns. The effects of these treatments are evident in Fig. 8, which displays simplified two-dimensional ^1H spectra obtained from basic pancreatic trypsin inhibitor, a protein with a molecular weight of approximately 6500. In the first instance, simple double-quantum filtering significantly attenuates the autocorrelated peaks on the diagonal, which include a strong signal from the solvent; whereas in the second instance, AX_3 topological filtering limits the spectrum primarily to signals from alanine residues, with the spin configuration $>CH–CH_3$ (*34*).

High-Resolution NMR in Inhomogeneous Magnetic Fields

The special properties of the extreme N-quantum transition find further application in a class of echo experiments developed to preserve both chemical shift and spin-spin interactions while overcoming the line broadening produced by a spatially inhomogeneous external magnetic field. These methods offer an additional level of control compared to that available in conventional echo experiments, in which the directions of all the magnetic fields responsible for the single-spin interactions, internal as well as external, are reversed, and the response of the system partitioned equally between the two conditions (*10*, *11*). The multiple-quantum adaptation uses instead two intervals unequal in length, monitoring first the N-quantum response for a time t_1 and then the single-quantum response for a time Nt_1 (*35*, *36*). Only the Zeeman interaction, represented by a spatially varying offset frequency $N\Delta\omega(\mathbf{r})$, influences the development of the system during the first period, since the N-quantum frequency is independent of the internal couplings. The Zeeman interaction is reversed in the second period, however, where it produces oscillations at the single-quantum frequency $-\Delta\omega$, and thus its effect is eliminated entirely when the signal is sampled after a rephasing period of length Nt_1. The signal observed at the peak of the echo is modulated by the chemical shift and spin-spin interactions normally present during the single-quantum refocusing interval, and may be Fourier-transformed to produce a

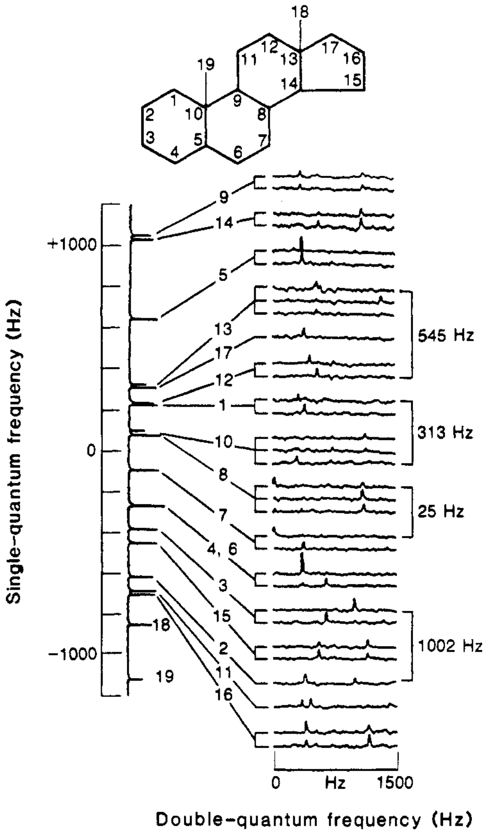

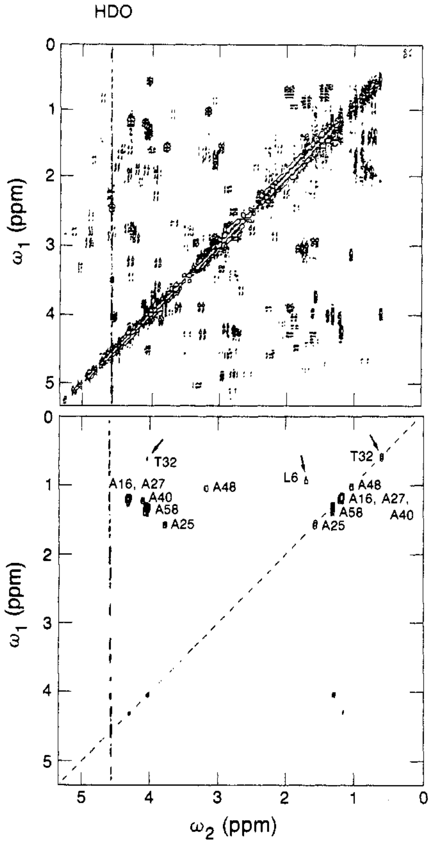

Fig. 7 (left). Elucidation of the carbon skeleton of an organic molecule by double-quantum filtering (*33*). The sections shown are taken from a two-dimensional, natural abundance ^{13}C spectrum that correlates two-quantum frequency components present during the evolution period with one-quantum frequency components present during the detection period. Every single-quantum resonance observed during t_2 originates from a double-quantum mode involving two J-coupled ^{13}C nuclei, which are sufficiently dilute to behave as an isolated subsystem of two spins. The single-quantum resonances of the members of each pair are identified by a common double-quantum frequency, equal to the sum of the chemical shifts of the two coupled nuclei. In this way all direct couplings between the carbon atoms are made clear, and the framework of the molecule is revealed. Connections between carbons 2-3, 7-8, 10-1, and 12-13 are indicated explicitly on this spectrum of 5α-androstane. [Courtesy of A. Bax, R. Freeman, T. Frenkiel (*33*) © 1981 American Chemical Society.] Fig. 8 (right). Two-dimensional correlated ^1H spectra of the aliphatic region of basic pancreatic trypsin inhibitor in D_2O shown as contour plots (*32*). At the top is a spectrum simplified by double-quantum filtering. The uncorrelated peaks on the diagonal, which include a solvent resonance at the position marked HDO, are attenuated considerably compared to the conventional spectrum. Below, the equivalent spectrum excited with an AX_3-selective preparation sequence contains peaks originating mainly from six alanine residues and one threonine residue. [Courtesy of M. H. Levitt and R. R. Ernst (*32*) © 1985 American Institute of Physics]

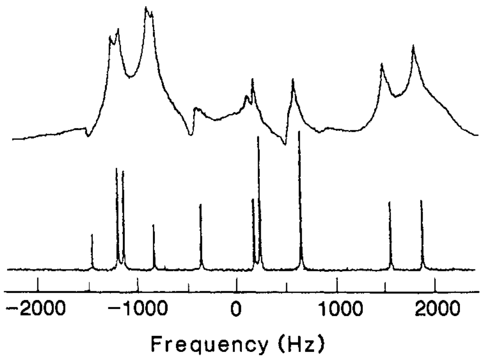

Fig. 9. Removal of inhomogeneous broadening by total spin coherence transfer echo spectroscopy. At the top is a conventional single-quantum ^{1}H spectrum of acetaldehyde in a nematic liquid crystal, broadened by more than 1 ppm owing to spatial inhomogeneity in the Zeeman field. Below is the N-quantum → 1-quantum echo spectrum, governed only by the chemical shift and spin-spin interactions, with line widths of 0.02 ppm (*35*). [Adapted from (*35*) with permission ©1981 American Chemical Society]

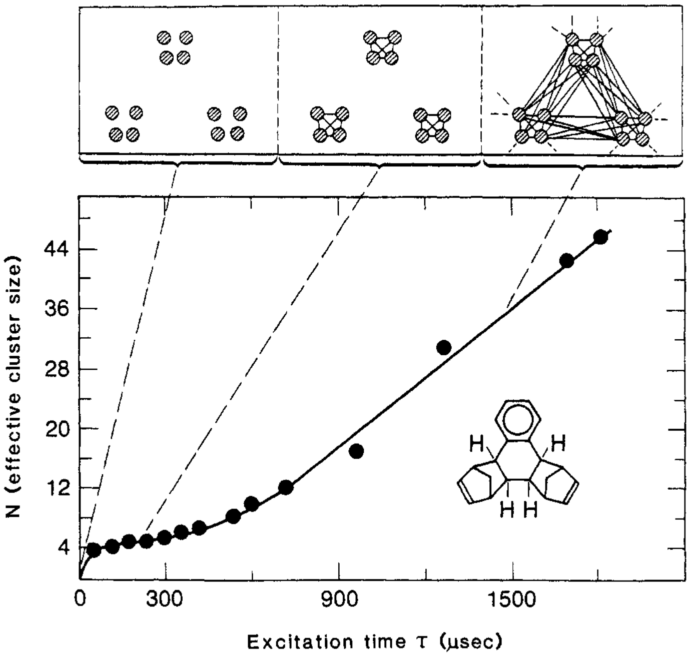

Fig. 10. Growth of a coupling network in a protonated solid, illustrated schematically (top) and experimentally (bottom) with a plot of $N(\tau)$ versus τ. The system is a polycrystalline sample of the molecule shown in the inset below, chlorinated at all unmarked carbon positions. The initial portion of the curve, up to approximately 400 μsec, arises mostly from intramolecular multiple-quantum events involving the four ^{1}H nuclei on individual molecules. Intermolecular dipole-dipole interactions become important after longer periods of excitation, and the effective size of the system grows well beyond the four-spin intramolecular cluster. [Courtesy of J. Baum]

homogeneously broadened spectrum in which the resonant frequencies are independent of the positions of the nuclei in the external field. An example of the effect is provided in Fig. 9, where a poorly resolved ^{1}H spectrum of partially oriented acetaldehyde obtained by conventional methods is contrasted with a sharp, chemically shifted spectrum obtained with the multiple-quantum echo experiment in the same inhomogeneous external field (*35*).

Multiple-Quantum Spectroscopy in Solids

Various forms of interspin communication, activated through the spin-spin couplings by mechanisms similar to those depicted in Fig. 2, provide the basis for collective action in coupled systems and therefore underlie all methods of multiple-quantum excitation. The development of the necessary multiple-body correlations in a collection of spins is a dynamic process that proceeds pair by pair, requiring in each instance a finite time for propagation. A crude physical picture, but one rooted in the time-dependent Schrödinger equation nonetheless, demands that two nuclei interact for a time inversely proportional to their mutual coupling frequency for the coupling to be effective; hence distant spins, linked by relatively weak local fields, need longer times to establish contact than do proximate spins. In general, extended periods of multiple-quantum excitation draw increasing numbers of spins into a network that can expand until all possible couplings have been exhausted (*23*, *37*). For species in isotropic or nematic phases, the ultimate size of the system is usually small, limited either to a few nuclei separated by three or four chemical bonds or to the nuclei on a single molecule. The situation is quantitatively different in rigid solids, however, where the dipole-dipole interactions, unhindered by motional averaging, exert their influence over long distances and connect all the nuclei without regard to molecules, functional groups, or other chemical subunits. As a result, a solid-state system is macroscopic in extent, essentially infinite, and prolonged multiple-quantum excitation promotes the formation of a continuously expanding network of correlated spins. This unbounded expansion with excitation time is mirrored in the multiple-quantum spectra by a continuous increase in the variance of the intensity distribution, which now yields a time-dependent effective size, $N(\tau)$. Solid-state spectra for which n exceeds 60, corresponding to multiple-quantum events involving hundreds of spins, have been reported recently for polycrystalline systems containing ^{1}H (*37*, *38*).

Multiple-quantum dynamics in solids are dominated initially by the largest couplings, which usually are associated with the shortest internuclear contacts. This dominance is soon lost in a system where the nuclei are distributed homogeneously but is retained in one where the nuclei are segregated into dilute, isolated clusters. When the separation between neighboring clusters is sufficient to inhibit intergroup communication over the time scale set by the multiple-quantum excitation, the limited set of large couplings continues to control the development of the system and thereby retards the growth of the effective size (*37*). These basic features of the dynamics are illustrated in Fig. 10, which is a plot of $N(\tau)$ versus τ obtained for a polycrystalline sample of 1,2,3,4-tetrachloronaphthalene-*bis*(hexachloropentadiene) adduct (*39*). The bulky chlorinated rings in this compound sharply reduce interactions between ^{1}H nuclei on different molecules and thus hold the effective size to 4 to 6 spins over the first 300 to 400 μsec of excitation. Nevertheless, long-range communication eventually takes over, and the number of connected spins grows swiftly once the intermolecular barrier is broken. Materials where the break between intracluster and intercluster coupling is even sharper have also been examined successfully by multiple-quantum NMR; notable examples include a study of the intermediate state assumed by acetylene when adsorbed on a surface of platinum (*40*) and an investigation of the sizes of hydrogen clusters in hydrogenated amorphous silicon (*41*).

Imaging of Solids by Multiple-Quantum Resonance

NMR imaging methods deliberately introduce gradients into the external field in order to render the resonant frequency of a nucleus dependent on its location in the sample. Thus labeled, the positions of the nuclei may be mapped out over a macroscopic distance to

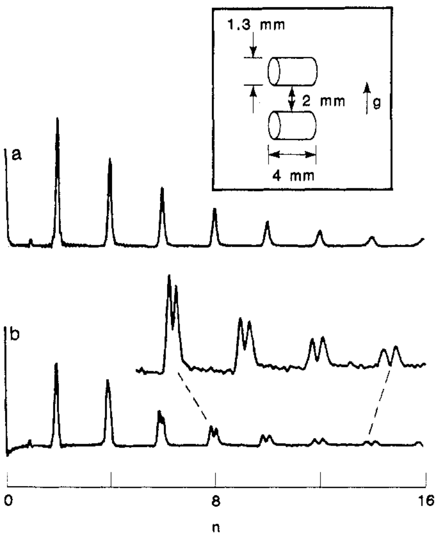

Fig. 11. Application of multiple-quantum NMR to imaging in solids. Multiple-quantum ^{1}H spectra of two cylindrical samples of polycrystalline adamantane, arranged as shown in the boxed diagram without (a) and with (b) a static gradient of 20 kHz/cm in the direction of the Zeeman field. The apparent n-fold intensification of the effect of the gradient, **g**, on an n-quantum spectrum is evident in the steady improvement in the resolution of the signal of the signals from the two plugs (*44*). [Reprinted from (*44*) with permission ©1984 Academic Press]

create an image of the spin density in the direction of the gradient (*42, 43*). The spatial resolution attainable in this fashion is limited by the magnitude of the internal fields and the strength of the gradient, however, since the extra field imposed within a volume must overwhelm any existing local fields if the region is to be labeled cleanly. This requirement is easily satisfied in isotropic systems (such as the mobile water molecules commonly used in medical imaging), where the strongest spin-1/2 interaction, the dipole-dipole coupling, is absent. When very strong nuclear dipolar fields are naturally present, though, as they generally are in a rigid solid, unrealistically large gradients may be needed to form an acceptable image.

The technical difficulties associated with the generation of powerful gradients are eased, however, when the methods of multiple-quantum spectroscopy are combined with the basic imaging experiment. The aim here is merely to exploit the n-fold amplification of any resonance offset to enhance both the effective strength of the gradient and its spatial resolving power correspondingly (*44*). The expected progressive improvement in resolution is demonstrated in Fig. 11 with a series of cross-sectional ^{1}H images of two cylindrical samples of adamantane placed in a gradient too small to distinguish conventional single-quantum signals from the two sites. Yet the same gradient can be used to produce a multiple-quantum image that is clearly resolved beginning with the $n = 10$ spectrum, where the apparent strength of the incremental field is increased tenfold. As a result, variations of the ^{1}H spin density over distances on the order of 1 mm, rather than 1 cm, are now discernible in the image.

Multiple-Quantum Relaxation and Correlated Motions

We conclude this brief survey of spectroscopic applications with a few comments concerning the processes by which a system of spins in a nonstationary multiple-quantum condition returns to equilibrium. In most instances several different relaxation mechanisms are operative simultaneously, each driven by the random fluctuations of a particular local field. These fluctuations reorient the spins and damp out the nonequilibrium oscillations, thus imparting finite widths to the resonances in the frequency domain. Consequently, analysis of the line widths in any NMR spectrum, single-quantum or multiple-quantum, promises to provide insight into the motions of the spins or their surroundings responsible for the fluctuations (*6, 7, 45, 46*). Since a multiple-quantum resonance in a coupled system requires the participation of more than one spin, however, its relaxation is sensitive to local field differences at all the nuclear sites concerned, and therefore provides a measure of the degree to which the internal motions are correlated (*47, 48*). This additional information helps complete the picture of microscopic structure and dynamics developed by NMR and may be used to characterize cooperative motions at selected sites in complex molecules.

REFERENCES AND NOTES

1. M. Mehring, *Principles of High Resolution NMR in Solids* (Springer-Verlag, Berlin, ed. 2, 1983), and references therein.
2. G. Bodenhausen, *Prog. Nucl. Magn. Reson. Spectrosc.* **14**, 137 (1981).
3. D. P. Weitekamp, *Adv. Magn. Reson.* **11**, 111 (1983).
4. G. Drobny, *Annu. Rev. Phys. Chem.* **26**, 451 (1985).
5. M. Munowitz and A. Pines, *Adv. Chem. Phys.* **66**, 1 (1985).
6. A. Abragam, *The Principles of Nuclear Magnetism* (Oxford Univ. Press, Oxford, 1963).
7. C. Slichter, *Principles of Magnetic Resonance* (Springer-Verlag, Berlin, ed. 2, 1978).
8. In restricting the treatment to systems of coupled spin-1/2 nuclei, we choose not to discuss multiple-quantum NMR in single-particle, multilevel systems of spin-I ($I \geqq 1$) nuclei, wherein the electric quadrupole coupling is the most important internal interaction. Notwithstanding the semantic differences between a group of interacting two-level systems and a single multilevel system, much of the picture developed for the spin-1/2 case is equally valid for quadrupolar nuclei.
9. S. W. Sinton, D. B. Zax, J. B. Murdoch, A. Pines, *Mol. Phys.* **53**, 333 (1984).
10. E. L. Hahn, *Phys. Rev.* **80**, 580 (1950).
11. H. Y. Carr and E. M. Purcell, *ibid.* **94**, 630 (1954).
12. U. Haeberlen, *High Resolution NMR in Solids: Selective Averaging, Adv. Magn. Reson., Suppl. 1* (Academic Press, New York, 1976).
13. W. S. Warren and A. Pines, *J. Am. Chem. Soc.* **103**, 1613 (1981).
14. W. P. Aue, E. Bartholdi, R. R. Ernst, *J. Chem. Phys.* **64**, 2229 (1976).
15. A. Wokaun and R. R. Ernst, *ibid.* **67**, 1752 (1977).
16. S. Vega, *ibid.* **68**, 5518 (1978).
17. S. Sinton and A. Pines, *Chem. Phys. Lett.* **76**, 263 (1980).
18. H. Hatanaka and T. Hashi, *J. Phys. Soc. Jpn.* **39**, 1139 (1975).
19. S. Vega and A. Pines, *J. Chem. Phys.* **66**, 5624 (1977).
20. A. Wokaun and R. R. Ernst, *Chem. Phys. Lett.* **52**, 407 (1977).
21. W. S. Warren, S. Sinton, D. P. Weitekamp, A. Pines, *Phys. Rev. Lett.* **43**, 1791 (1979).
22. W. S. Warren, D. P. Weitekamp, A. Pines, *J. Chem. Phys.* **73**, 2084 (1980).
23. J. B. Murdoch, W. S. Warren, D. P. Weitekamp, A. Pines, *J. Magn. Reson.* **60**, 205 (1984).
24. G. Bodenhausen, R. L. Vold, R. R. Vold, *ibid.* **37**, 93 (1980).
25. A. Bax, R. Freeman, S. Kempsell, *J. Am. Chem. Soc.* **102**, 4849 (1980).
26. G. Bodenhausen and C. M. Dobson, *J. Magn. Reson.* **44**, 212 (1981).
27. U. Piantini, O. W. Sørensen, R. R. Ernst, *J. Am. Chem. Soc.* **104**, 6800 (1982).
28. A. J. Shaka and R. Freeman, *J. Magn. Reson.* **51**, 169 (1983).
29. P. J. Hore, E. R. P. Zuiderweg, K. Nicolay, K. Dijkstra, R. Kaptein, *J. Am. Chem. Soc.* **104**, 4286 (1982); P. J. Hore, R. M. Scheek, A. Volbeda, R. Kaptein, J. H. van Boom, *J. Magn. Reson.* **50**, 328 (1982); P. J. Hore, R. M. Scheek, R. Kaptein, *ibid.* **52**, 339 (1983).
30. O. W. Sørensen, M. H. Levitt, R. R. Ernst, *J. Magn. Reson.* **55**, 104 (1983).
31. M. H. Levitt and R. R. Ernst, *Chem. Phys. Lett.* **100**, 119 (1983).
32. ———, *J. Chem. Phys.* **83**, 3297 (1985).
33. A. Bax, R. Freeman, T. A. Frenkiel, *J. Am. Chem. Soc.* **103**, 2102 (1981).
34. K. Nagayama, A. Kumar, K. Wüthrich, R. R. Ernst, *J. Magn. Reson.* **40**, 321 (1980); A. Bax and R. Freeman, *ibid.* **44**, 542 (1981).
35. D. P. Weitekamp, J. R. Garbow, J. B. Murdoch, A. Pines, *J. Am. Chem. Soc.* **103**, 3578 (1981).
36. J. R. Garbow, D. P. Weitekamp, A. Pines, *J. Chem. Phys.* **79**, 5301 (1983).
37. J. Baum, M. Munowitz, A. N. Garroway, A. Pines, *ibid.* **83**, 2015 (1985).
38. Y.-S. Yen and A. Pines, *ibid.* **78**, 3579 (1983).
39. J. Baum and A. Pines, *J. Am. Chem. Soc.*, in press.
40. P.-K. Wang, C. P. Slichter, J. H. Sinfelt, *Phys. Rev. Lett.* **53**, 82 (1984).
41. J. Baum, K. K. Gleason, A. Pines, A. N. Garroway, J. A. Reimer, *Phys. Rev. Lett.* **56**, 1377 (1986).
42. P. C. Lauterbur, *Nature (London)* **242**, 190 (1973).
43. L. Kaufman, L. E. Crooks, A. R. Margulis, Eds., *Nuclear Magnetic Resonance in Medicine* (Igaku-Shoin, New York, 1981); P. Mansfield and P. C. Morris, *NMR Imaging in Biomedicine, Adv. Magn. Reson., Suppl. 2* (Academic Press, New York, 1982); P. A. Bottomly, *Rev. Sci. Instrum.* **53**, 1319 (1982); E. R. Andrew, *Acc. Chem. Res.* **16**, 114 (1983).
44. A. N. Garroway, J. Baum, M. G. Munowitz, A. Pines, *J. Magn. Reson.* **60**, 337 (1984).
45. N. Bloembergen, E. M. Purcell, R. V. Pound, *Phys. Rev.* **73**, 679 (1948); R. K. Wangsness and F. Bloch, *ibid.* **89**, 728 (1953); F. Bloch, *ibid.* **102**, 104 (1956); A. G. Redfield, *IBM J. Res. Dev.* **1**, 19 (1957); *Adv. Magn. Reson.* **1**, 1 (1965).
46. R. A. Hoffman, *Adv. Magn. Reson.* **4**, 87 (1970); R. L. Vold and R. R. Vold, *Prog. Nucl. Magn. Reson. Spectrosc.* **12**, 79 (1978).
47. A. Wokaun and R. R. Ernst, *Mol. Phys.* **36**, 317 (1978).
48. J. Tang and A. Pines, *J. Chem. Phys.* **72**, 3290 (1980); J. Tang, thesis, University of California, Berkeley (1981) [Report LBL-13605 (Lawrence Berkeley Laboratory, Berkeley, CA, 1981)].
49. This work was supported by the Director, Office of Energy Research, Office of Basic Energy Sciences, Materials Science Division of the U.S. Department of Energy under contract DE-AC03-76SF00098.